Int. J. Heat Mass Transfer. Vol. 21, pp. 203–213. Pergamon Press 1978. Printed in Great Britain

LAMINAR FLOW STRUCTURE IN VERTICAL FREE CONVECTIVE CAVITIES

G. L. MORRISON and V. Q. TRAN
School of Mechanical and Industrial Engineering, University of N.S.W.,
Kensington, Australia 2033

(*Received* 29 *December* 1975 *and in revised form* 24 *May* 1977)

Abstract—This paper describes an investigation of the natural convective flow structure generated by heat transfer in a vertical rectangular cavity for aspect ratio of 5. Velocity profiles were measured at a Rayleigh number of 5×10^4 and the three dimensional flow structure determined. The effect of end wall conduction on the flow structure was investigated by varying the degree of insulation applied to the unheated walls.

The measurements show that end wall conduction affects the whole flow structure and thus may introduce significant deviations from the commonly assumed two dimensional conditions in the central section. Investigation of the three dimensional flow structure by laser-Doppler anemometry showed that the horizontal velocity component parallel to the heat conducting plates is small compared with the vertical component when the end walls are carefully insulated. However, when end wall insulation similar to that employed in many past heat transfer experiments is used, a strong three dimensional motion is produced.

The measured velocity distribution in the central sectional of the cell was compared with numerical and analytical predictions in the boundary layer regime.

NOMENCLATURE

A, Aspect ratio of cavity, H/L;
B, dimension of cavity in y-direction, horizontal and parallel to the heating plates;
g, acceleration due to gravity;
h, film coefficient of heat transfer;
H, height of cavity;
L, width of cavity;
Pr, Prandtl number, ν/α;
Ra, Rayleigh number based on the width of the cavity, $g\gamma\Delta TL^3/\alpha\nu$;
T_H, temperature of the hot plate;
T_c, temperature of the cold plate;
V_x, x-component of velocity;
V_y, y-component of velocity;
V_z, z-component of velocity;
V_x^*, non-dimensional x-component of velocity

$$\left[= V_x \Big/ \frac{\alpha}{L} Ra^{\frac{1}{4}} A^{\frac{1}{4}} \right];$$

V_y^*, non-dimensional y-component of velocity

$$\left[= V_y \Big/ \frac{\alpha}{L} Ra^{\frac{1}{4}} A^{\frac{1}{4}} \right];$$

V_z^*, non-dimensional z-component of velocity

$$\left[= V_z \Big/ \frac{\alpha}{L} Ra^{\frac{1}{4}} A^{\frac{1}{4}} \right];$$

x, distance from cold plate to hot plate;
y, horizontal distance along the plate;
z, distance from the bottom of the cavity;
x^*, y^*, z^*, dimensionless co-ordinates,

$$\frac{x}{L}, \frac{y}{B}, \frac{z}{H}.$$

Greek symbols

α, thermal diffusivity;
β, vertical temperature gradient;
γ, cubical thermal expansion coefficient;
ΔT, temperature difference;
ρ, density;
ν, kinematic viscosity;
ξ, scaled horizontal x co-ordinate

$$\left\{ = xRa^{\frac{1}{4}} \left[\frac{L}{H} \right]^{\frac{1}{4}} \frac{1}{L} \right\}.$$

1. INTRODUCTION

DESPITE considerable interest in natural convection within enclosed cavities there have been few measurements of fluid velocities generated by free convective heat transfer in such situations. Until recently most investigations have attempted to establish correlations for steady state heat transfer only, but with advances in computing power it is now possible to use numerical techniques to investigate the relative importance of factors effecting the heat transfer and flow structure without resorting to expensive experimental rigs. The first experimental investigation of heat transfer in cavities was reported in 1930 by Mull and Reiher [1] and the first detailed analytical investigation by Batchelor [2], who investigated both the heat transfer and flow structure in a long narrow cavity. Batchelor defined the various flow regimes and determined the parameters that govern the flow structure. For low Ra, Batchelor [2] determined that conduction is the sole means of heat transfer as convection is restricted to the top and bottom of the cavity. As Ra increases the convection effects propagate into the rest of the cavity; and for large Ra the flow consists

of a boundary layer surrounding a constant temperature core. By assuming that the temperature varies linearly across the cavity end walls, Batchelor [2] obtained a solution for both velocity and temperature distributions in large aspect ratio cavities ($H/L > 42$).

Subsequent studies by Eckert and Carlson [3], Elder [4], Gill [5] and Oshima [6] established that a vertical temperature gradient (β) exists in the centre of the cavity such at $\beta \cdot A \simeq$ constant for $Ra > 10^5$. Using this observation Elder [4] was able to show that the velocity profile in the centre of the cavity is given by

$$V_z = (2m^2 f/\beta Pr^2) \times [e^{-mx^*} \sin mx^* - e^{-m(1-x^*)} \sin m(1-x^*)] \quad (1)$$

where $4m^4 = \beta Ra$ and f was found experimentally to be approximately 0.25 for $Ra = 50000$ [4] and an asymptotic value of $f = 0.5$ was obtained for high Ra.

The first detailed velocity measurements were reported by Elder [4] who used medicinal paraffin and silicone oil as the working fluids. He used streak photographs produced by aluminium powder suspended in the fluid to measure velocities for Rayleigh numbers up to 10^8, aspect ratios from 1 to 60 and Prandtl numbers from 1100 to 2600. A series of vertical velocity profiles were obtained in the central region of the cavities. Elder's [4] results showed that the velocity profiles were not symmetrical about the centre line. Higher velocities and smaller wall layer thickness were observed in the flow near the hot wall, possibly as a result of the variation of fluid properties through the cavity. The cavities used by Elder [4] had an open upper surface so that thermocouples could be inserted to measure temperature distributions. The vertical end walls were made of glass and perspex for direct observation while the bottom wall was insulated.

Oshima [6] also measured heat transfer and flow structure in cavities with aspect ratios from 6 to 30 and for Rayleigh numbers up to 10^7. The cavities were constructed of pyrex-glass with water as the working fluid. Velocities were measured by observing small aluminium particles and a Mach-Zehnder interferometer was used to measure temperature. The temperature and velocity distributions were similar to those reported by Elder [4].

A further experimental study of natural convection with a stress on flow structure was made by Landis and Yanowitz [7] who investigated transient and steady state natural convection for Ra from 900 to 2×10^6 in an aspect ratio 20 cavity. Velocity profiles were obtained using a dye-tracing technique, and they observed that at steady state the maximum velocity adjacent to the hot wall was higher than the corresponding velocity near the cold wall at the same horizontal level. Subsequent theoretical studies by Gill [5] concur with Elder's [4] results that for a given Ra and Pr the core stream function and temperature depend only on the vertical co-ordinate. Gill [5] also developed the following approximate solution for the velocity distribution in the boundary layer regime.

$$V_Z = C^2 e^{-\zeta} \sin \zeta \quad (2)$$

where V_z is the vertical velocity and ζ is the characteristic horizontal x co-ordinate and

$$C^2 = \left[\frac{\gamma \cdot g \cdot \alpha}{\nu G}\right]^{\frac{1}{4}} \cdot \Delta T$$

with $G = 4\Delta T/H$.

As part of this analysis it was assumed that the thermal conditions on the top and bottom horizontal boundaries would only alter the solutions significantly in the immediate vicinity of these boundaries. Quon's [8] numerical investigations also indicated that the boundary conditions on the horizontal walls have little effect on the flow in the central region of the cell. Rubel and Landis [9] studied flows in an aspect ratio 5 cavity, using fluids with $Pr = 1$, 7 and 2000 in the range of $Ra = 6 \times 10^4$–3.6×10^5. The horizontal walls were assumed adiabatic. Vertical velocity distribution across the cavity at $z^* = 0.5$ was determined for $Pr = 2000$ and $Ra = 1.2$ and 5×10^5.

All the above studies were based on the assumption that the flow in the central region of the cavity is two dimensional. There have been some recent numerical studies of free convection in cavities that investigate the extent and effect of three dimensional motion in the cell due to end wall conduction, e.g. Mallinson [10], Mallinson and de Vahl Davis [11]. These studies indicate that a double spiral motion is established in the cell, however there have been few experimental investigations of the nature and extent of the three dimensional motion predicted by the numerical studies.

Many past experiments have been performed in cavities where end wall conduction was not properly controlled. (Elder [4], Oshima [6] and Eckert and Carlson [3] assumed $B \gg L$ so that the flow in the central vertical section could be considered two dimensional: the thermal effect of the vertical end walls was also disregarded. As the cavities in these experiments were made of either pyrex glass [6], perspex [4] or thin balsa wood [3] the flow structure in the central section may have been influenced by the three dimensional motion predicted in the numerical studies.

The effect of the horizontal boundaries was not investigated by Elder [4] and Oshima [6] since they used open-topped cavities in their studies. Also additional insulation was not used on the side boundaries of the cavities hence the influence of heat loss through the horizontal and vertical end boundaries was not investigated. It is the aim of the following experiments to determine if the flow in the centre of the cavity is affected by the type of conducting end walls that have been used in many flow visualisations and optical temperature measurement experiments and to compare the data with available analytical and numerical predictions.

The effect of horizontal boundary conditions on the flow and the resulting velocity distribution are also investigated experimentally.

2. EXPERIMENTAL APPARATUS

Figure 1(a) shows a vertical cavity with heat conducting side walls parallel to the yz plane and insulated vertical and horizontal end boundaries.

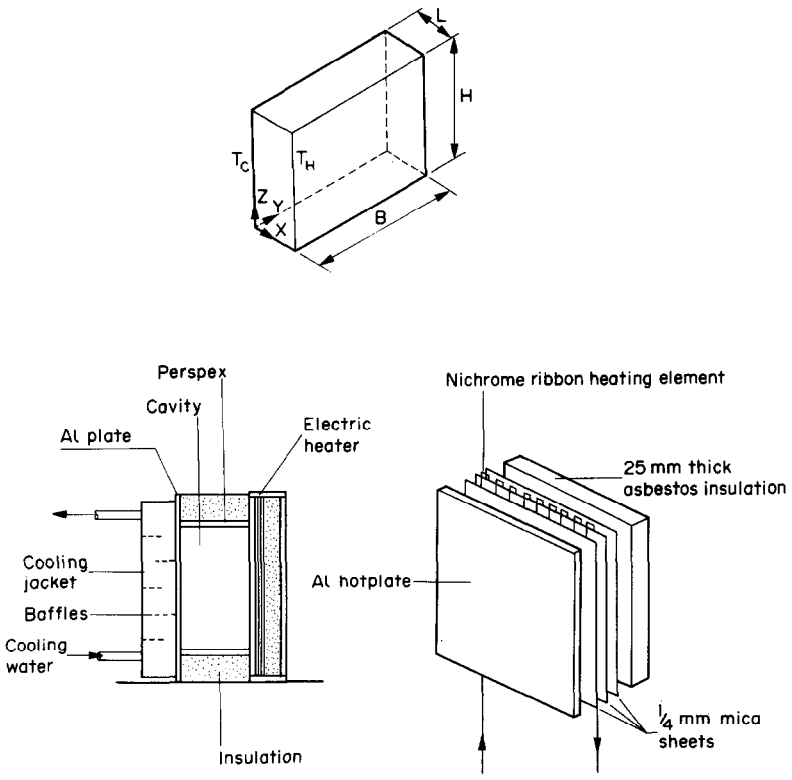

FIG. 1. Notation and test apparatus.

T_H and T_c denote the hot and cold plate temperatures, H, L and B are the cavity height, length and breadth.

The parameters governing the heat transfer are the Rayleigh number Ra, Prandtl number Pr and cell aspect ratios H/L and B/L.

The construction of the cavities and heat-transfer surfaces is shown in Fig. 1(b). The vertical heat-transfer plates were made of 12.7 mm thick aluminium. The hot plate was electrically heated by a series of nichrome ribbon strips which were separated from the back surface of the aluminium plate by a 0.25 mm mica sheet to avoid hot spots. The cold plate temperature was controlled by passing water from a temperature controlled bath through a 5 cm thick jacket as shown. The temperature of both plates was monitored by Chromel–alumel thermocouples mounted in blind holes drilled to within 0.5 mm of the inner surface of the heat conducting plates. All the thermocouple holes were filled with a mixture of aluminium powder and araldite to ensure uniform conduction in the plates. The heat-transfer surfaces were maintained at approximately isothermal condition with a maximum temperature variation over either plate of $\pm$ 0.25°C.

The heat-transfer surfaces were separated by cavities of 12.7 mm thick perspex and the heat loss through the end walls controlled by adding a 35 mm layer of polyurethane foam outside the perspex walls. The temperature difference between the cavity and the surrounding atmosphere varied between 10 and 15°C. Tests with the additional insulation were made to determine the effect of end wall conduction on the flow structure. A series of perspex end walls were employed to test the effect of aspect ratio on the flow structure. As the tests required a long settling period the equipment was mounted in an air-conditioned room ($4 \times 4 \times 10$ m).

A laser doppler anemometer was used to measure the velocity field since a transducer does not have to be inserted into the flow and thus flow disturbances are avoided. Also the response of a laser-Doppler anemometer is independent of the properties and temperature of the fluid. The system senses velocity in one direction only and thus is ideally suited for measurement in three dimensional flow. As very low velocities were anticipated the instrumentation system was developed to handle velocities down to 0.25 mm/s [12]. A typical optical configuration and signal processing system is shown in Fig. 2. To produce a continuous doppler signal the flow was seeded with tobacco smoke. Errors in velocity measurement due to misalignment of the laser sensitivity vector were minimised by careful alignment of the optics [12].

As a frequency shifting device was not used, the laser system had a 180° uncertainty in flow direction. To aid the interpretation of results in three dimensional situations the flow patterns produced by the smoke particles were observed and photographed.

The flow structure in both the horizontal and vertical planes was determined by illuminating a thin segment of the smoke in the cavity using the laser light source and a cylindrical lens to produce a thin plane of light. The main motion in the vertical plane was investigated by passing the light sheet through the top wall of the

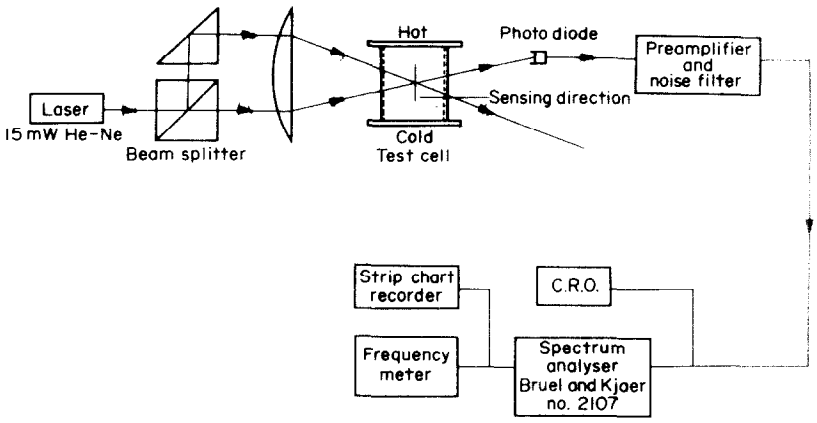

FIG. 2. Laser-Doppler anemometer and instrumentation.

cavity and photographing from the side. For the tests with additional insulation the top or side layers were removed only briefly to avoid disturbing the flow. As only a low intensity light was used, exposure times up to 1.5 min were needed.

To ensure equilibrium conditions the cavity was left to stabilise for several hours after the smoke had been introduced. This was particularly important when the foam insulation was not used as in this case it took approximately 2 h for the end region flow to stabilize. The temperature difference between the heat transfer plates was fixed at 10°C and the plate separation $L = 40\,\text{mm}$ ($Ra = 5 \times 10^4$). This Rayleigh number was selected so that the secondary transitions in the vertical motion as observed by Elder [4] would not be present. The cavity aspect ratio was 5 in both the horizontal and vertical planes (H/L and B/L).

3. RESULTS

3.1. *Two dimensional flow regime*

(a) *Perspex walled cell.* The vertical velocity (V_z) profile was measured at the mid-height of the cavity ($z^* = 0.5$) for a series of positions between the cavity centre and the vertical end walls, see Fig. 3. These results indicate that the vertical flow is uniform over the central segment of the cavity $0.2 < y^* < 0.8$. Thus the end wall affects the flow for a distance slightly greater than the separation of the heated plates (corresponds to $y^* = 0.2$). The surprising characteristic of these measurements is that the profiles are not symmetric about the midplane, $x^* = 0.5$. The velocity near the cold plate is 15% less than the velocity at a corresponding point near the hot plate. This lack of symmetry has been mentioned in other investigations [4, 7] in cells with similar end boundaries and attributed to fluid property variations with temperature. The fluid property which varies most with temperature and has the greatest effect on Ra is the fluid viscosity. However this is unlikely to be the cause as the same lack of symmetry has been observed in experiments using oils and water [4, 7], which have the opposite temperature dependence of viscosity of the air medium used in these experiments.

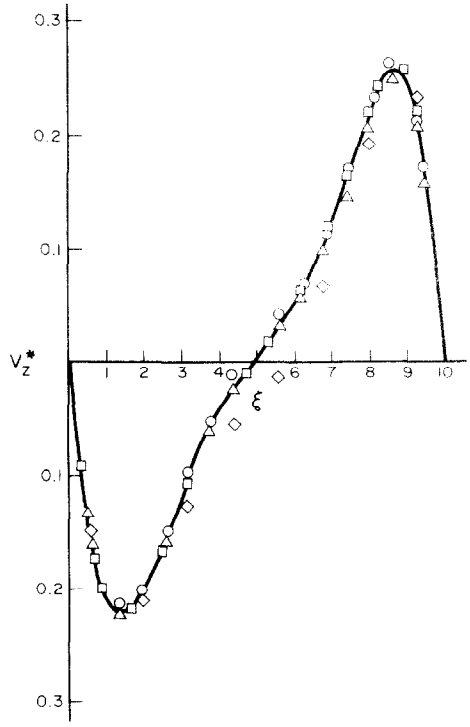

FIG. 3. Vertical velocity profile ($Z^* = 0.5$, perspex end walls) ○, $Y^* = 0.5$; □, $Y^* = 0.3$; △, $Y^* = 0.2$; ◇, $Y^* = 0.1$.

For the 10°C temperature difference used in these tests a first order estimate of the difference in volume flux due to density changes indicate a volume flow rate difference of less than 2% compared to the observed difference of more than 10%. As the flow is bounded these results imply that there is a significant three dimensional flow in the cavity.

(b) *Insulated endwalls.* The effect of end wall heat loss on the vertical profile was investigated by repeating the measurements after an additional 35 mm of foam insulation was added outside the four perspex boundaries. Figure 4 shows that with additional end insulation the vertical velocity profile is invariant between $y^* = 0.1$ and 0.9. The variation of the peak velocity with distance into the cell is shown in Fig. 5.

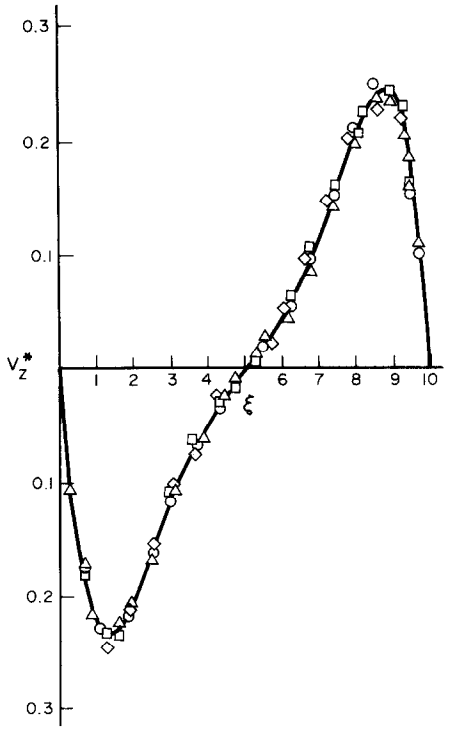

FIG. 4. Vertical velocity profile ($Z^* = 0.5$, insulated end walls) ○, $Y^* = 0.5$; □, $Y^* = 0.3$; △, $Y^* = 0.2$; ◇, $Y^* = 0.1$.

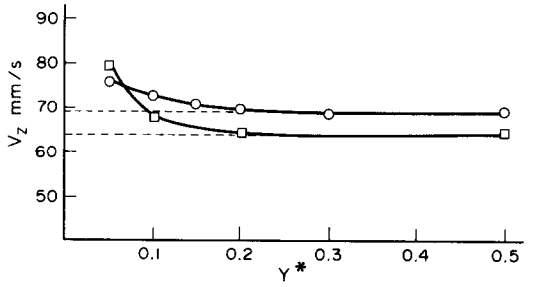

Fig. 5. Peak velocity V_Z near cold wall. ○, insulated end walls; □, Perspex end walls.

The flow region influenced directly by end wall conduction is thus reduced from $y^* = 0.2$ to $y^* = 0.1$ by the addition of the insulation. These results indicate that the additional insulation not only changes the extent of the uniform central section of the flow but also has a significant effect on the velocity profile in the central region of the cavity. Figure 4 shows that profiles in the insulated cell are almost symmetric about the centre line. The difference in the volume flux near the hot and cold walls is 2% for the insulated end wall condition compared to 10% for the perspex end walls. The volume flux difference for the insulated cavity is only slightly larger than the estimated difference due to density variations across the cavity. Further evidence of the effect of end wall conduction on the flow structure in the centre of the cavity is shown by a comparison of the vertical velocity profiles at various heights in the mid-plane of the cavity, Fig. 6.

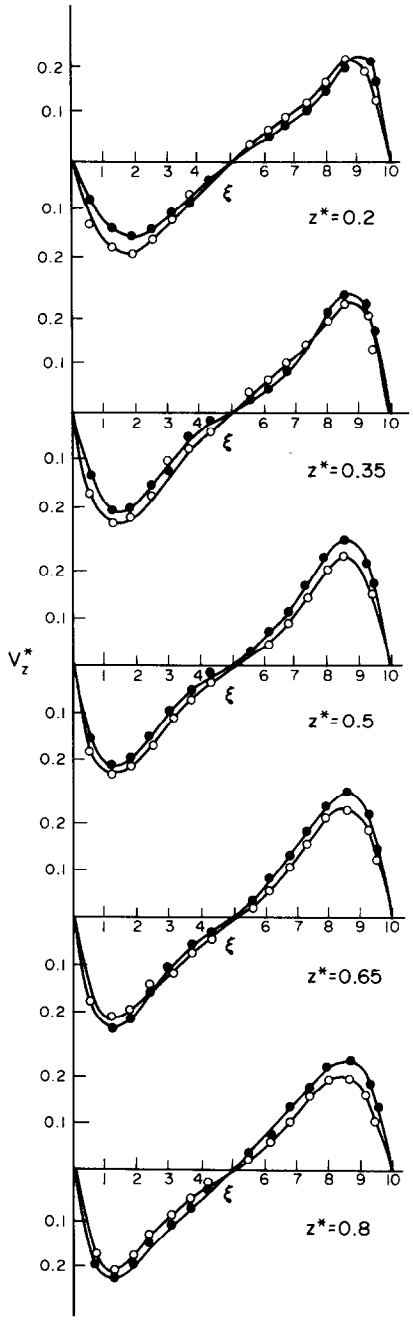

FIG. 6. Vertical velocity profile ($Y^* = 0.5$). ●, Perspex end walls; ○, insulated end walls.

3.2. *Three dimensional flow structure*

The three dimensional structure of the flow in the perspex walled cavity inferred from the vertical velocity measurements was investigated by using the laser anemometer to measure the horizontal velocity component parallel to the vertical heat transfer surface (V_y).

In the central zone of the cell V_y was found to be less than the minimum detectable velocity which was 0.25 mm/s. However, measurements at positions in the mid-horizontal plane but off the vertical central plane indicated a strong horizontal velocity as shown in

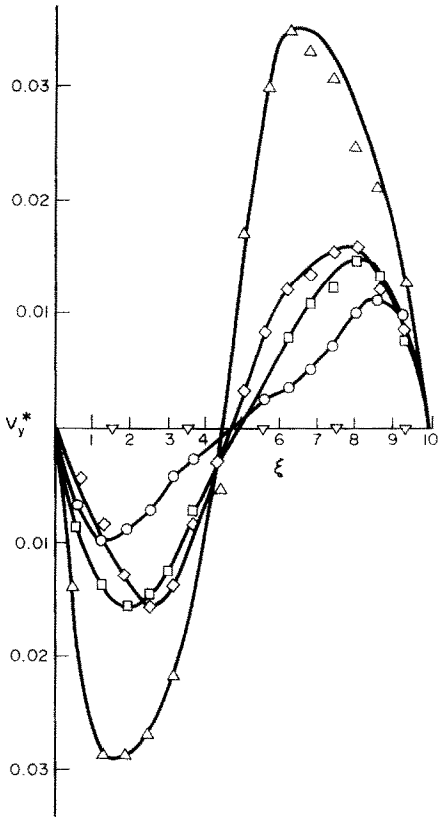

FIG. 7. Horizontal velocity V_y^* ($Z^* = 0.5$, perspex end walls). ◇, $Y^* = 0.05$; Δ, $Y^* = 0.1$; □, $Y^* = 0.25$; ○, $Y^* = 0.4$; ▽, $Y^* = 0.5$

Fig. 7. The velocity profiles were the same on either side of the midplane and indicate that as the flow is convected up the hot plate it also develops a velocity component directed towards the centre line. On the cold side the fluid tends to move away from the central plane as it moves down the cold wall.

These profiles indicate that after passing over the top (or bottom) boundary of the cavity the flow develops a horizontal velocity component directed towards the end walls (or central plane). As the laser system could only indicate the magnitude of the velocity, the flow directions were determined by visual tracing of smoke particles. To further aid the interpretation of the flow structure, photographic records (1 to 2 min time exposure) were taken of the flow pattern produced by smoke particles in both the horizontal and vertical planes. Figure 8 shows the vertical flow structure in the central region of the perspex walled cell. The patterns show a single cell structure with a slight inclination of the core region towards the top of the hot wall.

Figure 9(a) shows the flow pattern in the horizontal mid-plane. The extent of the end wall region is shown by the darker areas at either end of the cavity. Although it is not clear in the photograph a weak rotating structure with a vertical axis could be seen near $y^* = 0.1$ to $y^* = 0.15$. The patterns shown in Fig. 9 were recorded 4 h after the smoke was added to the cell, during this time most of the particles trapped in the end region had settled out onto the end wall of the

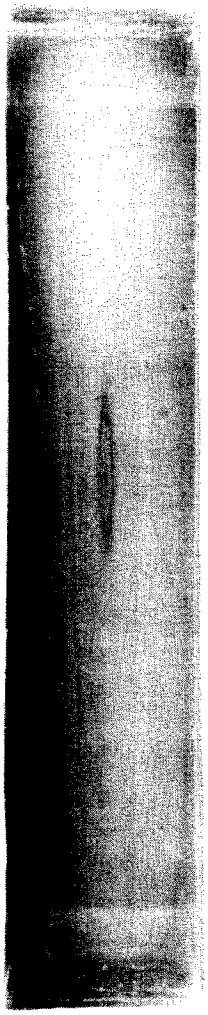

FIG. 8. Streamline pattern in vertical central plane (uninsulated cavity). Hot wall on LHS.

cavity. The lighter region of the plate shows the central core section of the cell where most particles remained. The interesting feature in this photograph is the dividing line across the centre of the cavity at right angles to the heat-transfer plates. This line coincides with the region of zero horizontal velocity (V_y) found during the velocity measurements. The dark central line parallel to the heated walls is a section of the core of the main flow shown in Fig. 8. Figure 9(b) shows the horizontal pattern at three-quarters of the cell height ($z^* = 0.75$). The central line indicating the core of the main flow has disappeared but the dividing line was found to exist over the full height of the cell indicating that the three dimensional flow is divided about the vertical mid-plane at right angles to the heat transfer plates.

Measurements of the velocity component (V_x) at right angles to the heating plates indicated that motion in the x direction only occurs at the top and bottom of the cell where the main flow passes from the hot to cold wall, and in the vertical end wall region. Figure 10 shows the distribution of this velocity component at various positions at mid-height in the vertical end wall

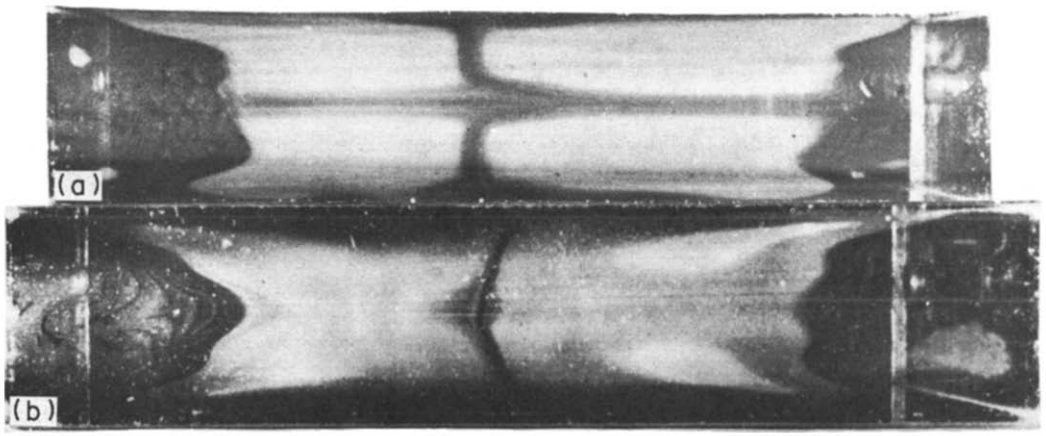

FIG. 9. Flow pattern in horizontal planes. (a) $Z^* = 0.5$, (b) $Z^* = 0.75$. $Ra = 5 \times 10^4$; $A = 5 \times 5$; average end wall heat-transfer coefficient = 1 W/m^2 °C.

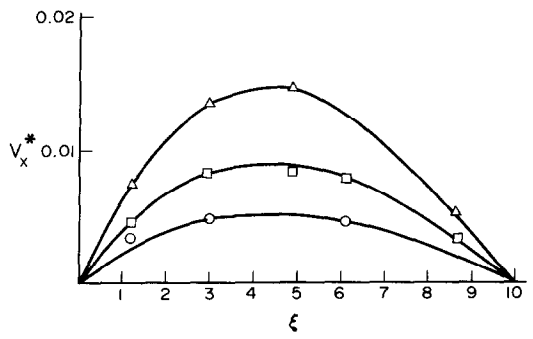

FIG. 10. Horizontal velocity distribution V_x^* in central plane of perspex walled cavity, $Z^* = 0.5$. Δ, $Y^* = 0.05$; □, $Y^* = 0.1$; ○, $Y^* = 0.15$.

region. No velocity component normal to the heat-transfer walls was detected in the central flow region, i.e. $V_x = 0$ for $0.25 < y^* < 0.75$ and $z^* = 0.5$.

The velocity measurements and flow patterns indicate that the flow is divided by the central vertical plane at right angles to the hot and cold plates as shown in Fig. 11. If the horizontal velocity is such that the fluid enters the end wall region (as appears to happen close to the heated walls) it passes across the vertical end wall and onto the opposite heat conducting plate.

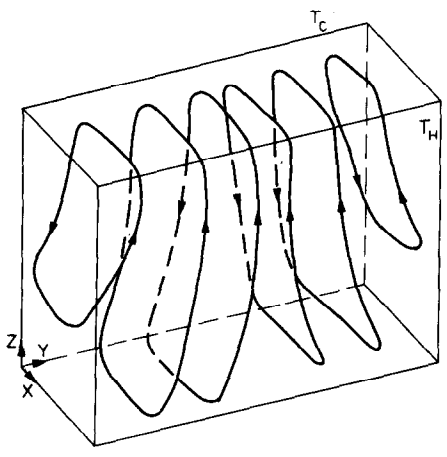

FIG. 11. Three dimensional flow structure.

3.3. *Flow structure for adiabatic end wall condtions*

The effect of additional end wall insulation on the three dimensional flow structure was examined using flow visualisation in the horizontal mid-plane, see Fig. 12(a). This photograph shows that a significant change in the flow structure occurs when the end wall conduction is reduced. The region of direct influence of the end walls has reduced substantially (as the vertical velocity profiles indicate) and does not appear to exist, however a change in the smoke patterns was observed in the end region but was too diffuse to appear in the photograph. The main aspect of this pattern is that although the extent of direct end wall influence has been reduced there is still a three dimensional flow that propagates to the centre of the cell. The herringbone pattern down the centre indicates a spiralling motion from the end walls towards the centre and then a reverse spiral outside the central zone.

Figure 12(b) shows the horizontal pattern at $z^* = 0.75$ (at three-quarters cell height). The position of the transverse dividing line between the two halves of the cell was found to be very sensitive to slight differences in end conditions and in Fig. 12(b) it is slightly off centre.

After the two converging flows have met at the centre the fluid spirals out and returns to the end walls. Attempts to measure the secondary velocity components in this insulated cavity were unsuccessful as all velocities were less than or close to the minimum resolution of the anemometer. Thus with additional insulation the three dimensional velocity components are an order of magnitude lower than for perspex end wall conditions, however the three dimensional flow still propagates to the centre of the cavity.

The flow structure in the vertical plane for completely insulated end walls is shown in Fig. 13. The spiralling motion implied from Fig. 12 is clearly shown. This type of motion has been predicted numerically by Mallinson and de Vahl Davis [11] and has also been observed by Mallinson and Graham [13] for an aspect ratio of 5 with end wall heat loss controlled by dummy air cavities around the central cavity.

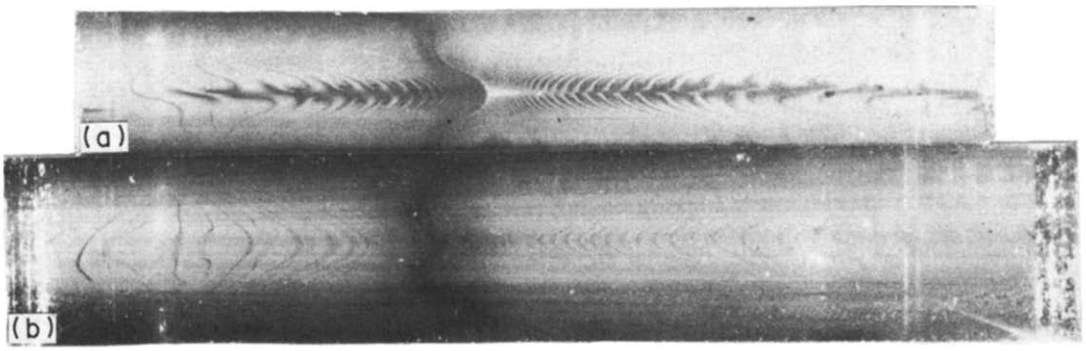

FIG. 12. Flow pattern in horizontal planes. (a) $Z^* = 0.5$, (b) $Z^* = 0.75$. $Ra = 5 \times 10^4$; $A = 5 \times 5$; average end wall heat-transfer coefficient = 0.3 W/m^2 °C.

The centre of rotation of the vertical flow patterns shown in Figs. 8 and 13 is positioned slightly above ($z^* \approx 0.53$) the geometric centre. This lack of symmetry may be due to variation of fluid properties throughout the cavity, it does not appear to be due to different heat loss through the top and bottom walls as the same lack of symmetry was observed for both the insulated and uninsulated cavities. Asymmetry of the flow has also been observed in other experimental studies [3, 4, 7, 13].

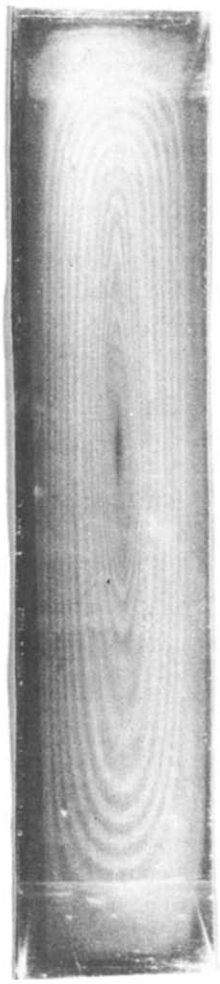

FIG. 13. Streamline pattern in vertical central plane (insulated cavity). Hot wall on LHS.

3.4. *Relative influence of vertical and horizontal boundaries*

The results reported in Section 3.1 have shown that the flow structure is significantly influenced by the degree of insulation applied to the four end boundaries. However Gill's [5] analysis and Quon's [8] numerical predictions indicated that the vertical boundary layer flow in the centre of the cell is not influenced by the thermal condition of the horizontal boundaries.

To check the relative influence of the vertical and horizontal boundaries, the flow patterns were investigated when each pair of the end boundaries were insulated in turn. Observation of the three dimensional flow patterns in the cell showed that the shift in the flow structure observed in the previous section could be produced by applying insulation to the vertical end walls alone. When the horizontal boundaries were insulated and the vertical boundaries left uninsulated a change of flow pattern was observed but it was still essentially the same as the uninsulated case.

3.5. *Comparison of experimental, analytic and numerical results*

As there is no equivalent data on horizontal velocity components only the vertical velocity measurements of this investigation will be compared with other published data. Figures 14 and 15 compare data from the following reports at midheight of the cavity ($z^* = 0.5$) and $z^* = 0.2$ and 0.8. The upper and lower comparison levels were selected to be outside the similar central zone $0.35 < z^* < 0.65$.

All the results are scaled using Gill's [5] parameters of characteristic velocity $\alpha/L\,[Ra/(L/H)]^{\frac{1}{2}}$ and characteristic length $L/[Ra/(L/H)]^{\frac{1}{4}}$. Gill [5] predicted that the resulting profile should be independent of Ra and A provided the boundary-layer thickness in the centre of the cavity is small compared with the cavity width. The necessary criterion for this condition is that $11.5\,Ra^{-\frac{1}{4}}\,A^{\frac{1}{4}} < 1$, this factor is listed in Table 1.

Figure 14 compares measured and predicted profiles at the midheight of the cavity. There is good agreement between the data from this investigation and Elder's [4] $Ra = 4 \times 10^5$ results, while Oshima's [6] data for $Ra = 5 \times 10^6$ is approximately 10% higher.

The numerical predictions of Quon [8] and Rubel and Landis [9] also show good agreement with the

Table 1

Authors	Ra	A	Pr	$(11.5\,Ra^{-\frac{1}{4}}\cdot A^{\frac{1}{2}})$
Authors' Data	50000	5	0.71	1.1
Rubel and Landis [9]	300000	5	2000	0.73
Elder [4]	400000	18	1000	0.94
Gill [5]	400000	18	1000	0.94
Quon [8]	800000	1	7.14	0.384
Oshima [6]	5000000	8	7	0.41

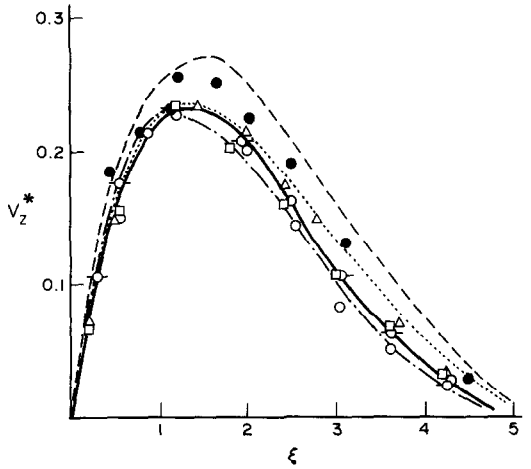

FIG. 14. Comparison of experimental data with analytical and numerical predictions at $Z^* = 0.5$. ○,-○-, Authors' results (hot and cold wall respectively); ●, Oshima's results; □, Elder's results; △, Rubel and Landis' numerical prediction; ——, Quon's numerical prediction; – – –, Gill's analytical prediction; ·····, Gill's corrected results; —·—, Elder's analytical prediction.

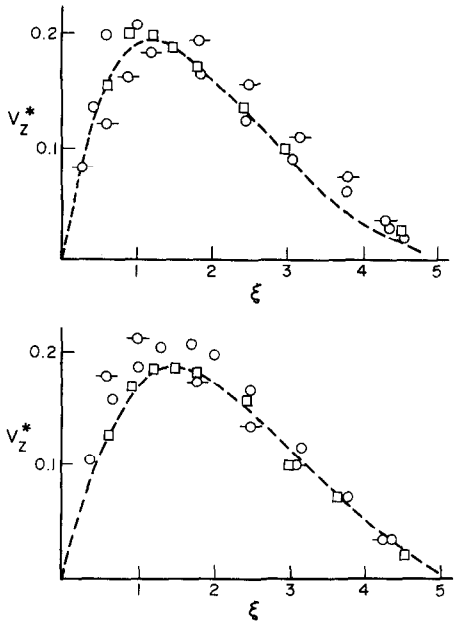

FIG. 15. Comparison of experimental data with analytical prediction at $Z^* = 0.2$ and $Z^* = 0.8$ respectively. ○, -○-, Authors' data (hot and cold wall respectively); □, Elder's data; – – –, Gill's prediction.

experimental results. Gill's [5] analytic prediction also overestimates the velocity by up to 20%, however this discrepancy can be overcome by correcting the constant C in Gill's [5] equation (6.18) as discussed by Quon [8]. Comparison of the form of Gill's [5] equation with the data in Fig. 14 shows that the value of the constant C as given by Gill [5] is 10% high. The adjusted form of Gill's equation is also shown in Fig. 14.

The results in Fig. 14 indicate that Gill's [5] velocity and length scales are valid for $Ra < 5 \times 10^6$ and all Prandtl numbers that were tested ($0.7 < Pr < 2000$).

Comparison of results near the top and bottom boundaries are given in Fig. 15. The results of this investigation show a marked difference in the shape of the hot and cold side profiles. Gill's [5] modified equation is shown to underestimate the velocities and does not indicate the relative difference between the flow profiles on the hot and cold boundaries.

4. CONCLUSIONS

The vertical flow structure is uniform over a wide central section of the cavity. The extent of uniformity depends on the vertical end wall conditions and varies from $0.2 < y^* < 0.8$ for a 12 mm thick perspex walled cavity exposed to the atmosphere ($h_{av} = 1.0$ W/m^{2}C) to $0.1 < y^* < 0.9$ for an insulated cavity ($h_{av} = 0.3$W/m^{2}C). End wall conduction influences the symmetry of the velocity profiles in the centre of the cell such that the peak velocity near the hot wall is significantly higher than the corresponding value near the cold wall. For the high conductivity end wall conditions used in one of these tests and in many other experiments, the laser anemometer measurements showed that a strong three dimensional motion is generated by the vertical end wall heat loss. Thus the asymmetry observed in other investigations [4, 7] may have been due to three dimensional effects and not fluid property variations. The observation that the velocity profiles in the central section of the cavity were independent of the horizontal boundary conditions employed, e.g. open topped tank (Elder [4]), perspex walls and insulated perspex walls (this investigation) demonstrated that the horizontal boundaries exert little influence on the vertical flow pattern. Comparison of the results in Figs. 14 and 15 shows that Gill's [5] boundary layer regime scaling produces good correlation of both numerical and experimental results for Rayleigh number range $5 \times 10^4 < Ra < 5 \times 10^6$ and aspect ratio $1 < A < 18$.

REFERENCES

1. W. Mull and H. Reiher, Der warmeshutz von luftschichten, *Beih. Gesundh-Ing* Reihe 1 **28** (1930).
2. G. K. Batchelor, Heat transfer by free convection across a closed cavity between vertical boundaries at different temperatures, *Q. Appl. Maths.* **12**(3), 209–233 (1954).
3. E. R. G. Eckert and W. O. Carlson, Natural convection in an air layer enclosed between two vertical plates with different temperatures, *Int. J. Heat Mass Transfer* **2**, 106–120 (1961).
4. J. W. Elder, Laminar free convection in a vertical slot, *J. Fluid Mech.* **23** (1), 77–98 (1965).
5. A. E. Gill, The boundary-layer regime for free convection in a rectangular cavity, *J. Fluid Mech.* **26**(3), 515–536 (1966).
6. Y. Oshima, Experimental studies of free convection in a rectangular cavity, *J. Phys. Soc. Japan* **30**(3), 872–882 (1971).
7. F. Landis and H. Yanowitz, Transient natural convection in a narrow vertical cell, in *Proceedings of the Third International Heat Transfer Conference*, Vol. 2, pp. 139–151. A.I.Ch.E., New York (1966).
8. C. Quon, High Rayleigh number convection in an enclosure—a numerical study, *Physics Fluids* **15**, 12–19 (1972).
9. A. Rubel and F. Landis, A numerical study of natural convection in a vertical rectangular enclosure, Int. Symp. High Speed Computing in Fluid Dynamics, *Physics Fluids Suppl.* II **12**, 208–213 (1969).
10. G. D. Mallinson, Natural convection in enclosed cavities, Ph.D. thesis, University of N.S.W. (1973).
11. G. D. Mallinson and G. de Vahl Davis, The method of the false transient for the solution of coupled elliptic equations, *J. Comp. Physics* **12**, 435–461 (1973).
12. G. L. Morrison and V. Q. Tran, Low velocity limits of a laser doppler anemometer, School of Mech. & Ind. Engng, University of N.S.W., Report No. 1974/FMT/8 (1974).
13. G. D. Mallinson and A. D. Graham, Experimental visualization of three dimensional natural convection, in *Proceedings of the fifth Australasian Conference on Hydraulics and Fluid Mechanics*, Vol. 2, pp. 323–330, University of Canterbury, Christchurch, New Zealand (1974).

STRUCTURE D'ECOULEMENT LAMINAIRE DE CONVECTION NATURELLE DANS DES CAVITES VERTICALES

Résumé—On décrit une expérimentation sur la convection naturelle dans une cavité rectangulaire et vertical de rapport de forme égal à 5. On mesure les profils de vitesse à un nombre de Rayleigh de 5×10^4 et on détermine la structure tridimonsionnelle. On étudie l'effet de bord par conduction sur la structure de l'écoulement, en faisant varier l'isolation des parois non chauffées.

Les mesures montrent que la conduction affecte toute la structure d'écoulement et ceci peut introduire une différence notable avec les conditions bidimensionnelle dans la section centrale. Une observation par l'anémométrie laser Doppler montre que la composante horizontale de vitesse, parallèle aux plaques conductrices, est faible en comparaison avec la composante verticale quand les parois limites sont isolées avec soin. Néanmoins lorsque l'isolation est semblable à celle couramment réalisée dans des expériences antérieures, on produit un mouvement fortement tridimensionnel.

On compare la distribution expérimentale de vitesse, dans la section centrale de la cellule, aux prévisions numériques et analytiques en régime de couche limite.

LAMINARE STRÖMUNGSFORM BEI VERTIKALER FREIER KONVEKTION IN HOHLRÄUMEN

Zusammenfassung—Es wird über eine Untersuchung der Strömungsform bei natürlicher Konvektion infolge Wärmeübertragung in senkrechten Hohlräumen (Seitenverhältnis: 5) berichtet. Bei einer Rayleighzahl von $5 \cdot 10^4$ wurden Geschwindigkeitsprofile gemessen und die dreidimensionale Strömungsform bestimmt. Durch Variation des Isolationsgrades der ungeheizten Wände wurde der Einfluß der Wärmeleitung durch die Seitenwände (end wall) auf die Strömungsform untersucht. Die Messungen zeigen, daß die Wärmeleitung durch die Seitenwände (end wall) die Struktur der Gesamtströmung beeinflußt und in der Mitte des Hohlraums zu einer deutlichen Abweichung gegenüber den allgemein angenommenen zweidimensionalen Bedingungen führt. Untersuchungen der dreidimensionalen Strömungsform mit Hilfe der Laser-Doppler-Anemometrie zeigen, daß die horizontale Geschwindigkeitskomponente, sie ist parallel zu den wärmeleitenden Platten, klein ist im Vergleich zur vertikalen Komponente, wenn die Seitenwände (end walls) sorgfältig isoliert sind. Wenn die Isolation der Seitenwände (end wall) so ausgeführt wird, wie in vielen früheren Wärmeübertragungsuntersuchungen, stellt sich eine starke dreidimensionale Bewegung ein. Die gemessene Geschwindigkeitsverteilung in der Mitte der Zelle wurde mit numerischen und analytischen Lösungen für den Grenzschichtbereich verglichen.

О СТРУКТУРЕ ЛАМИНАРНОЙ СВОБОДНОЙ КОНВЕКЦИИ В ВЕРТИКАЛЬНЫХ ПОЛОСТЯХ

Аннотация — Исследуется структура конвективного движения в вертикальной прямоугольной полости при отношении сторон, равном 5. Измерялись профили скорости при числе Релея $5 \cdot 10^4$ и определялась трехмерная структура потока. Изучалось влияние теплопроводности торцевой стенки на структуру течения путем изменения степени изоляции ненагреваемых стенок.

Измерения показывают, что теплопроводность торцевой стенки оказывает влияние на структуру всего потока и таким образом может вызвать существенное отклонение от обычно принимаемых двумерных условий в центральной части полости. Исследование трехмерной структуры потока с помощью лазерного допплеровского анемометра показано, что горизонтальная компонента скорости, параллельная теплопроводящим стенкам, невелика по сравнению с вертикальной компонентой, когда торцевые стенки тщательно изолированы. Однако, в случае изоляции торцевой стенки в той степени, как это было сделано во многих ранее проведенных экспериментах по теплообмену, возникает сильное трехмерное движение.

Проведено сравнение измеренного профиля скорости в центральной части полости с численными и аналитическими расчетами, выполненными для пограничного слоя.